

Constraints on Evolutionary Properties of GHz Peaked Spectrum Galaxies

S. Tinti¹ and G. De Zotti^{2,1}

¹ SISSA/ISAS, Via Beirut 4, 34014, Trieste, Italy

² INAF, Osservatorio Astronomico, Vicolo dell'Osservatorio 5, 35122, Padova, Italy

...

Abstract. We have used the available samples of Gigahertz Peaked Spectrum (GPS) galaxies to investigate their evolution properties in the framework of the “youth” scenario. Care was taken to properly allow for the different selection criteria used to define the samples. We find that the observed redshift and peak frequency distributions can be satisfactorily accounted for in terms of simple luminosity evolution of individual sources, along the lines discussed by Fanti et al. (1995) and Begelman (1996, 1999), although the derived parameter values have large uncertainties due to ambiguities in the selection of GPS sources and to the incompleteness of redshift measurements. However the simplest self-similar model, whereby the evolution is controlled only by the radial profile of the density of the ambient medium is not good enough and one additional parameter needs to be introduced. The fit requires a decrease of the emitted power and of the peak luminosity with source age or with decreasing peak frequency, at variance with the Snellen et al. (2000) model. On the other hand, our analysis confirms the rather flat slope of the luminosity function, found by Snellen et al. (2000) who also report indications of a high luminosity break, not required by the data sets we have used. Our results suggest that the GPS galaxies are the precursors of extended radio sources with luminosities below the break of the luminosity function. No cosmological evolution of the GPS galaxy population is required by presently available data.

Key words. galaxies: active – radio continuum: galaxies

1. Introduction

Several lines of evidence increasingly point to Gigahertz Peaked Spectrum (GPS) sources (see O’Dea 1998 for a comprehensive review) being extremely young. Spectral age constraints, energy supply arguments and, most convincingly, VLBI kinematic studies, are all consistent with the current radio activity in these objects having turned on less than about 1000 years ago (Conway 2002), although in some cases there is evidence that this is not the first instance of activity, but sources appear to have been re-activated after a period of quiescence (Baum et al. 1990), perhaps by effect of merger activity (Tingay et al. 2003). These sources thus offer the exciting opportunity of studying radio sources in early stages of development.

There is a clear anti-correlation between the peak (turnover) frequency, ν_p , and the projected linear size of GPS sources (Fanti et al. 1990; O’Dea & Baum 1997). Although this anti-correlation does not necessarily define the evolutionary track, a decrease of the peak frequency as the emitting blob expands is indicated, suggesting a scenario whereby GPS sources evolve into Compact Steep Spectrum (CSS) sources and, finally, into the classical

large scale radio sources (Fanti et al. 1995; Readhead et al. 1996; Begelman 1996; Snellen et al. 2000).

The self-similar evolution model by Begelman (1996, 1999) imply that the evolution of the radio power as the source expands, depends on the radial profile of the external density. To test this scenario and to constrain the birth rates and the evolutionary properties of these sources, detailed comparisons of the model predictions with survey data are necessary. An exploratory study in this direction was presented by De Zotti et al. (2000), who showed that this kind of models may account for the observed counts, redshift and peak frequency distributions of the samples then available, but for rather unexpected values of the parameters.

Since then, new important surveys of GPS sources have been published, extending the coverage of the peak frequency-redshift plane. The Dallacasa et al. (2000) and Bolton et al. (2004) samples comprise sources with high turnover frequencies (called High Frequency Peakers, HFPs), which are presumably the youngest. Snellen et al. (2002) and Edwards & Tingay (2004) selected samples of southern GPS sources, thus improving the sky coverage. Snellen et al. (2004) focussed on the relatively rare low- z sources. The first year WMAP survey (Bennett et

al. 2003b) has provided a complete sample of over 200 sources with simultaneous flux density measurements at 4 frequencies (22.8, 33.0, 40.7, 60.8, and 93.5 GHz), that can be exploited to search for extreme GPS sources, peaking at mm wavelengths.

Moreover, the variability study of the Dallacasa et al. (2000) sample, carried out by Tinti et al. (2005), has shown that most HFP candidates classified as quasars are most likely blazars caught by during a flare of a highly self-absorbed component dominating the emission, while candidates classified as galaxies are consistent with being bona fide HFPs. Polarization measurements (Dallacasa et al., in preparation) lend further support to this conclusion. Torniainen et al. (2005) from a study of the long term variability of 33 objects previously classified as GPS or HFP sources, mostly identified with quasars and mostly peaking above 5 GHz, concluded that only 5 keep the GPS properties over time. Clearly, a serious blazar contamination of GPS samples may lead astray analyses of their statistical properties.

In view of these new data, the previous conclusions on the evolution of the GPS population need to be reconsidered in depth. In this paper we present a new analysis, still in the framework of Begelman's (1996, 1999). Since, as mentioned above, there are strong evidences that samples of GPS sources identified as quasars are heavily contaminated by flaring blazars, we confine our analysis to GPS galaxies. Our reference evolutionary scenario is briefly described in Sect. 2, in Sect. 3 we give an account of the data sets we use, in Sect. 4 we analyze the effect of the different selection criteria adopted to define the samples, in Sect. 5 we present our results, in Sect. 6 we summarize and discuss our main conclusions.

We have adopted a flat Λ CDM cosmology with $\Omega_\Lambda = 0.73$ and $H_0 = 70 \text{ km s}^{-1} \text{ Mpc}^{-1}$ (Bennett et al. 2003a).

2. The evolutionary scenario

Following De Zotti et al. (2000), we make the following assumptions:

1. The initial radio luminosity function (in units of $\text{Mpc}^{-3} \text{ d log } L_i^{-1}$) is described by a power law:

$$n(L_i) \propto \left(\frac{L_i}{L_\star} \right)^{-\beta}, \quad L_{i,\min} \leq L_i \leq L_{i,\max}, \quad (1)$$

where L_i is the luminosity before self-absorption.

2. In the GPS phase, the properties of the sources are determined by the interaction of a compact, jet-driven, overpressured, non thermal radio lobe with a dense interstellar medium (Begelman 1996, 1999; Bicknell et al. 1997); the timescale of the interaction is very short in comparison with the cosmological-expansion timescale, so that the luminosity evolution of individual sources occurs at constant z . As the radio lobe expands in the surrounding medium, the emitted radio power varies with the source age, τ , as $L_i \propto \tau^{-\eta}$, and its linear size l varies as $l \propto \tau^\epsilon$. If the density of the

surrounding medium scales with radius as $\rho_e \propto r^{-n}$, we have (Begelman 1996, 1999) $\eta = (n+4)/[4(5-n)]$ and $\epsilon = 3/(5-n)$. The Begelman's dependence of the radio power on source age assumes that the synchrotron emission is dominated by the high pressure region close to the head of the jet. Alternatively, Snellen et al. (2000) and Alexander (2000) assume that the emission comes from the full volume of the expanding cocoon, so that $\eta = (8-7n)/4(5-n)$. In Begelman's model the luminosity decreases with increasing source size for $n \geq 0$. On the other hand, according to Snellen et al. (2000) and Alexander (2000) the radio luminosity increases as $l^{2/3}$ if $n = 0$ (i.e. within the galaxy core radius) and then decreases as $l^{-0.5}$ as the density profile steepens to $n = 2$ at larger radii. Evolutionary tracks where the luminosity increases within the core radius and then decreases in a falling atmosphere in the power-diameter plane are also presented by Carvalho & O'Dea (2003) based on the results of a series of hydrodynamical simulations. There is a clear anti-correlation between intrinsic turnover frequency, ν_p , and linear size (O'Dea & Baum 1997): $\nu_p \propto l^{-\delta}$, with $\delta \simeq 0.65$. It follows that ν_p scales with time as $\nu_p \propto \tau^{-\lambda}$, with $\lambda = \delta\epsilon$.

3. The spectra of GPS sources are described by:

$$L_\nu = L_p \times \begin{cases} (\nu/\nu_p)^{\alpha_a} & \text{if } \nu < \nu_p \\ (\nu/\nu_p)^{-\alpha} & \text{if } \nu > \nu_p \end{cases} \quad (2)$$

with $\alpha_a = 0.8$ and $\alpha = 0.75$, the mean values found by Snellen et al. (1998b).

As the radio lobe expands, the peak luminosity L_p varies as the consequence of the variation of both the emitted radio power and of ν_p . Hence:

$$L_p(\nu_p) = L_{p,i} \tau^p = L_{p,i} \left(\frac{\nu_p}{\nu_{p,i}} \right)^{-p/\lambda} = L_{p,i} \left(\frac{\nu_p}{\nu_{p,i}} \right)^{\eta/\lambda - \alpha} \quad (3)$$

with $L_{p,i}(z) \propto L_i(z)$ and $p = -\eta + \alpha\lambda$.

If the birth rate of GPS sources is constant on time scales much shorter than the cosmological-expansion timescale, the peak luminosity function per unit $\text{d log } L_p$ is:

$$n(L_p) \propto L_p^{1/p}. \quad (4)$$

Also, since, in this case, the *comoving* number of sources of age τ within $\text{d}\tau$ is simply proportional to $\text{d}\tau$ and $\text{d}\tau/\text{d}\nu_p \propto (\nu_p/\nu_{p,i})^{-(1+1/\lambda)}$, the epoch dependent luminosity function at a given frequency ν ($\text{Mpc}^{-3} \text{ d log } L_\nu^{-1} \text{ GHz}^{-1}$) writes:

$$n(L_\nu, \nu_p, z) = n_0 \left(\frac{L_{p,i}(L_\nu, \nu_p)}{L_\star(z)} \right)^{-\beta} \left(\frac{\nu_p}{\nu_{p,i}} \right)^{-(1+1/\lambda)}, \quad (5)$$

where $L_\star(z)$ is the redshift-dependent normalization luminosity. We have assumed luminosity evolution and adopted a very simple parameterization for it:

$$L_\star(z) = L_0 \times \begin{cases} (1+z)^k & \text{if } z < z_c \\ (1+z_c)^k & \text{if } z > z_c \end{cases} \quad (6)$$

The redshift z_c at which luminosity evolution levels off is a model parameter. We have normalized monochromatic luminosities to $L_0 = 10^{32} \text{ erg s}^{-1} \text{ Hz}^{-1}$.

The luminosity function at a frequency ν_2 is related to that at a frequency ν_1 by:

$$n(L_{\nu_2}) = n(L_{\nu_1}) \times \begin{cases} (\nu_2/\nu_1)^{-\alpha_a} & \text{if } \nu_1 < \nu_2 < \nu_p \\ (\nu_1/\nu_p)^{\alpha_a} (\nu_2/\nu_p)^{\alpha} & \text{if } \nu_1 < \nu_p < \nu_2 \\ (\nu_2/\nu_1)^{\alpha} & \text{if } \nu_p < \nu_1 < \nu_2 \end{cases} \quad (7)$$

The number counts per steradian of GPS sources brighter than S_{ν} at the frequency ν , with an observed peak frequency $\max(\nu, \nu_{p,\min}) < \nu_{p,0} < \nu_{p,\max}$ are given by

$$N(>S_{\nu}; \nu_{p,0} > \nu) = \int_0^{\min[z_f, z_m(S_{\nu})]} dz \frac{dV}{dz} \times \\ \times \int_{\max[\nu_{p,\min}(1+z), \nu(1+z)]}^{\min[\nu_{p,\max}(1+z), \nu_{p,i}]} d\nu_p \times \\ \times \int_{\log L_{\min}(S_{\nu}, z, \nu_p)}^{\log L_{\max}(z)} d \log L_{\nu} n(L_{\nu}, \nu_p, z), \quad (8)$$

where z_f is the redshift of formation of the first GPS sources, z_m is the maximum redshift at which sources can have a flux $\geq S_{\nu}$, L_{\min} is the minimum luminosity of a source of given z and ν_p yielding a flux $\geq S_{\nu}$, dV/dz is the *comoving* volume element within a solid angle ω :

$$\frac{dV}{dz} = \frac{c}{H_0} \omega \frac{d_L^2}{(1+z)^2 E(z)} \quad (9)$$

$d_L(z)$ being the luminosity distance:

$$d_L(z) = \frac{c}{H_0} (1+z) \int_0^z \frac{dz'}{E(z')} \quad (10)$$

$$E(z) \equiv (\Omega_M (1+z)^3 + \Omega_{\Lambda})^{1/2}. \quad (11)$$

The flux density at the frequency ν is related to the rest-frame luminosity L_{ν} by:

$$S_{\nu} = \frac{L_{\nu} K(z)}{4\pi d_L^2} \quad (12)$$

$$K(z) = (1+z) \frac{L_{\nu(1+z)}}{L_{\nu}}. \quad (13)$$

$K(z)$ being the K-correction.

Similarly, the number counts of GPS sources with an observed peak frequency $\nu_{p,\min} < \nu_{p,0} < \min(\nu, \nu_{p,\max})$ are given by

$$N(>S_{\nu}; \nu_{p,0} < \nu) = \int_0^{\min[z_f, z_m(S_{\nu})]} dz \frac{dV}{dz} \times \\ \times \int_{\nu_{p,\min}(1+z)}^{\min[\nu(1+z), \nu_{p,\max}(1+z), \nu_{p,i}]} d\nu_p \times \\ \times \int_{\log L_{\min}(S_{\nu}, z, \nu_p)}^{\log L_{\max}(z)} d \log L_{\nu} n(L_{\nu}, \nu_p, z), \quad (14)$$

Table 1. Summary of GPS samples.

Sample	S_{\lim} Jy	ν_o GHz	area deg 2	ν_p^{\min} GHz	ν_p^{\max} GHz	$N_{\text{tot}}^{\text{gal}}$
HFP	0.3	4.9	15840	5.34	11.1	5
Stan	1.0	5.0	24600	0.4	4.9	19
B_SA	0.025	15.0	176	3.43	127.0	10
B_SB	0.060	15.0	70	3.29	10.3	0
Snel	0.018	0.325	522	1.0	5.7	14
CORA	0.1	1.4	2850	0.460	2.3	6
Park	0.5	2.7	12802	0.4	5.0	48
Edwa	0.95	5.0	16414	0.7	7.5	9

The distribution of observed peak frequencies per unit $d\nu_{p,0}$ in a flux limited sample, $\mathcal{N}(\nu_{p,0}; > S_{\nu})$, is given by:

$$\mathcal{N}(\nu_{p,0}; > S_{\nu}) = \int_0^{\min[z_f, z_m(S_{\nu}, \nu_{p,0})]} dz \frac{dV}{dz} \times \\ \times \int_{\log L_{\min}(S_{\nu}, z, \nu_{p,0}(1+z))}^{\log L_{\max}(z, \nu_{p,0}(1+z))} d \log L_{\nu} n[L_{\nu}, z, \nu_{p,0}(1+z)]. \quad (15)$$

3. GPS samples

There is no clear-cut definition of GPS sources and different criteria have been adopted for identifying them. On the other hand, we need to combine at least the most reliable samples to gather enough data for a meaningful analysis to be possible. We now describe the samples used and the corrections applied to make them as homogeneous as possible. The main properties of the samples are summarized in Table 1, where HFP, Stan, B_SA, B_SB, Snel, CORA, Park, and Edwa denote, respectively, the samples by Dallacasa et al. (2000, HFP sample), by Stanghellini et al. (1998), by Bolton et al. (2004, 9C samples A and B), by Snellen et al. (1998, as revised by Snellen et al. 2000, faint WENSS sample), by Snellen et al. (2004, CORALZ sample), by Snellen et al. (2002, Parkes sample), and by Edwards & Tingay (2004, ATCA sample).

3.1. The 9C samples

Bolton et al. (2004) selected two complete samples of sources from the first three regions of the 9C survey: a deeper sample (sample A), complete to 25 mJy and containing 124 sources over a total area of 176 square degrees; a shallower sample (sample B), complete to 60 mJy, comprising 70 sources in an area of 246 square degrees, including the area covered by sample A. Restricting the sample B to the 70 sq. deg. not overlapping the sample A we are left with 31 sources. Simultaneous observations of each source were made at frequencies of 1.4, 4.8, 22 and 43 GHz with the VLA and at 15 GHz with the Ryle Telescope. In addition, 51 sources were observed within a few months at 31 GHz with the Owens Valley Radio Observatory (OVRO) 40m telescope. Sources with spectral index between 1.4 and 4.8 GHz $\alpha_{1.4}^{4.8} < -0.1$ ($S_{\nu} \propto \nu^{-\alpha}$) were referred to as

Table 2. GPS candidates from Bolton et al. 2004.

Name		S_p (mJy)	ν_p (GHz)
J0003 + 2740 ^A	Q?	76 ± 1	5.4 ± 0.1
J0003 + 3010 ^A	G?	0.55	60 ± 3
J0010 + 2854 ^A	Q?		10.3 ± 0.3
J0012 + 3353 ^A	G?	0.50	100 ± 5
J0012 + 3053 ^A	G?	0.45	199 ± 12
J0020 + 3152 ^A	G?	0.45	27 ± 1
J0020 + 3152 ^A	-	1.1	20 ± 4
J0024 + 2911 ^A	Q?		43.8 ± 0.8
J0024 + 2911 ^A	Q?		4.91 ± 0.09
J0032 + 2758 ^A	G	0.51	42 ± 2
J0032 + 2758 ^A	G		34.4 ± 0.4
J0919 + 3324 ^B	G?	0.35	10.3 ± 0.5
J0925 + 3127 ^B	G?	0.26	135 ± 2
J0931 + 2750 ^B	G?	0.49	169 ± 3
J0935 + 2917 ^A	Q?		3.29 ± 0.06
J0936 + 3207 ^A	G?	0.49	47.3 ± 0.9
J0936 + 3207 ^A	G	0.20	8.3 ± 0.3
J0936 + 2624 ^B	Q?		14 ± 1
J0940 + 2603 ^B	G?	0.37	179 ± 18
J0945 + 2603 ^B	G?		6.1 ± 0.8
J0945 + 3534 ^B	Q?		413 ± 8
J0952 + 3512 ^B	Q?		4.0 ± 0.2
J0955 + 3335 ^B	Q?		427 ± 8
J1506 + 4239 ^A	G?	0.38	107 ± 2
J1506 + 4239 ^A	G		5.9 ± 0.2
J1517 + 3936 ^A	G?	0.38	766 ± 19
J1517 + 3936 ^A	G		14 ± 1
J1521 + 4336 ^A	Q?		0.46
J1521 + 4336 ^A	Q?		21 ± 3
J1526 + 3712 ^A	G?	0.61	431 ± 10
J1526 + 3712 ^A	G?		6.2 ± 0.2
J1526 + 4201 ^A	G?	0.61	74 ± 2
J1526 + 4201 ^A	G		6.9 ± 0.3
J1526 + 4201 ^A	G		8.1 ± 0.2
J1528 + 3816 ^A	G?	0.36	67 ± 1
J1528 + 3816 ^A	G?		26 ± 5
J1530 + 3758 ^A	G?	0.52	80 ± 3
J1530 + 3758 ^A	G		3.43 ± 0.06
J1540 + 4138 ^A	G?	0.19	141 ± 3
J1540 + 4138 ^A	G		8.8 ± 0.2
J1550 + 4536 ^A	G?	0.17	62 ± 1
J1550 + 4536 ^A	G		3.5 ± 0.07
J1554 + 4350 ^A	-	0.50	45.0 ± 0.8
J1554 + 4348 ^A	Q?	0.36	10.9 ± 0.3
J1556 + 4259 ^A	Q?		63 ± 1
J1556 + 4259 ^A	Q?		3.7 ± 0.1
J1556 + 4259 ^A	Q?		94 ± 4
J1556 + 4259 ^A	Q?		4.3 ± 0.2

GPS sources. The adopted criterion implies that sources peaking at $\nu_p \gtrsim 5$ GHz were preferentially (but not exclusively) selected. With this definition, there are 22 GPS sources in sample A (14 galaxies, 6 quasars and 2 unidentified sources) and 8 (4 galaxies and 4 quasars) in the (redefined) sample B.

In order to estimate the peak flux densities, S_p , and frequencies, ν_p , of the sources, we have fitted the radio spectra with the hyperbolic function used by Tinti et al. (2005):

$$\log(S) = \log(S_p) + b - [b^2 + c^2(\log \nu - \log \nu_p)^2]^{1/2}. \quad (16)$$

The best fit values of ν_p and S_p , obtained minimizing the chi-square function with the Minuit package (CERN libraries), are reported with their errors in column 4 and 5 of Table 2.

No redshift measurements are available for these sources. However, as shown by Snellen et al. (1996, 2002), GPS galaxies show a well defined R -band Hubble diagram, with a low dispersion. In terms of Gunn r magnitudes, Snellen et al. (1996) found a best fit relation:

$$r = 22.7 + 7.4 \log(z). \quad (17)$$

Table 3. The HFP galaxy sample. The * denotes an empty field, which was attributed $z = 1.5$.

Name	z	ν_p GHz
0428+3259	0.3	7.3
0655+4100	0.02156	7.8
1407+2827	0.0769	5.34
1511+0518	0.084	11.1
1735+5049	1.5*	6.4

The conversion from the Kron-Cousins R_c magnitudes measured by Bolton et al. (2004) to the Gunn r magnitudes was made taking $r = R_c + 0.3$ (Fukugita et al. 1995). The redshift estimates are given in Table 2. We do not count as galaxies the optically point-like objects, classified as G? by Bolton et al. (2004) because of their red colours ($O - R \geq 1.6$): if they were bright galaxies at the redshifts estimated from Eq. (17) they should be resolved. This leaves 10 GPS galaxies in sample A and zero in sample B (see Table 1).

It is important to note that other criteria for selecting GPS samples include tighter constraints on the low- and/or high-frequency spectral indices. The effect of the different selection criteria is discussed in Sect. 4.

3.2. The HFP sample

The bright HFP sample by Dallacasa et al. (2000) was selected by cross-correlating the 87GB (Gregory et al. 1996) sources with $S_{4.9\text{GHz}} \geq 300$ mJy with the NVSS catalogue (Condon et al. 1998) at 1.4 GHz and picking out those with inverted spectra ($\alpha < -0.5$, $S \propto \nu^{-\alpha}$). It was then “cleaned” by means of simultaneous multifrequency VLA observations, leaving 55 sources whose single-epoch radio spectrum peaks at frequencies ranging from a few GHz to about 22 GHz. The sample of HFP candidates comprises 11 galaxies (including a type 1 Seyfert), 36 quasars, and 8 still unidentified sources (Dallacasa et al. 2002), over an area of 15,840 deg².

Although there are, in this sample, some sources with $\nu_p < 4.9$ GHz, the selection criterion biases the sample against such values of ν_p in a way that we are unable to quantify. Therefore we have chosen to confine ourselves to sources with $\nu_p > 4.9$ GHz. Moreover we have excluded from the sample the objects with 4.9 GHz flux densities smaller than the completeness limit of 300 mJy when were they re-observed by Dallacasa et al. (2000) and Tinti et al. (2005). After having applied these additional constraints, we are left with 5 HFP galaxies, listed in Table 3.

3.3. The faint GPS sample from WENSS

The selection of this sample is described in detail in Snellen et al. (1998). Snellen et al. (2000) applied stricter criteria allowing a better control of selection effects; they

Table 4. The faint GPS galaxies from WENSS. The * denotes empty fields, which were attributed $z = 1.5$. Values of z with 3 significant digits are spectroscopic, the others are photometric estimates.

Name	z	ν_p GHz
B0400+6042	1.5*	1.0
B0436+6152	1.5*	1.0
B0535+6743	1.5	5.7
B0539+6200	1.4	1.9
B0830+5813	0.093	1.6
B1525+6801	1.1	1.8
B1551+6822	1.3	1.5
B1557+6220	0.9	2.3
B1600+7131	1.5*	1.7
B1622+6630	0.201	4.0
B1655+6446	1.5*	1.0
B1841+6715	0.486	2.1
B1942+7214	1.1	1.4
B1946+7048	0.101	1.8

Table 5. The bright GPS galaxies from Stanghellini et al. (1998). The * denotes photometric redshift estimates.

Name	z	ν_p GHz
0019-000	0.305	0.8
0108+388	0.669	3.9
0316+161	1.2*	0.8
0428+205	0.219	1.0
0500+019	0.583	2.0
0710+439	0.518	1.9
0941-080	0.228	0.5
1031+567	0.459	1.3
1117+146	0.362	0.5
1323+321	0.369	0.5
1345+125	0.122	0.6
1358+624	0.431	0.5
1404+286	0.077	4.9
1600+335	1.1*	2.6
1607+268	0.473	1.0
2008-068	0.7*	1.3
2128+048	0.99	0.8
2210+016	1.0*	0.4
2352+495	0.237	0.7

kept only the 14 objects with inverted spectra between 325 and 5 GHz, and with 325 MHz flux densities > 20 mJy, over an area of 522 deg 2 . The redshift of identified sources, all classified as galaxies, had to be estimated from their optical magnitudes, using Eq. (17). For the 4 unidentified sources, also assumed to be galaxies, a redshift of $z=1.5$ was assumed. The relevant data for all the 14 objects are given in Table 4.

Table 6. The ATCA sample of GPS galaxies from (Edwards & Tingay 2004). The * denotes empty fields, which were attributed $z = 1.5$.

Name	z	ν_p GHz
J0241-0815	0.004	7.5
J1543-0757	0.172	0.7
J1658-0739	1.5*	4.8
J1726-6427	1.5*	1.1
J1723-6500	0.014	2.7
J1744-5144	1.5*	1.0
J1939-6342	0.183	1.4
J2257-3627	0.006	2.7
J2336-5236	1.5*	1.1

3.4. The bright GPS sample

Stanghellini et al. (1998) selected candidate radio bright GPS sources from the Kühr et al. (1981) catalogue ($S_{5\text{GHz}} \geq 1$ Jy), over an area of about $24,600$ deg 2 . The sample was then cleaned by means of multifrequency VLA and WSRT observations, supplemented with literature data. They picked out GPS candidates with a turnover frequency between 0.4 and 6 GHz, and an optically thin spectral index $\alpha_{\text{thin}} > 0.5$ ($S_\nu \propto \nu^{-\alpha}$), beyond the peak. The final complete sample consists of 33 GPS sources, 19 of which are identified with galaxies. Four galaxies do not have spectroscopic redshift; estimates by Snellen et al. (2000) from their optical magnitudes [Eq. (17)] are denoted by a * in Table 5, where the relevant data for the 19 galaxies are listed.

3.5. The ATCA GPS sample

Edwards & Tingay (2004) have used data from an Australia Telescope Compact Array (ATCA) program of multi-frequency, multi-epoch monitoring of the portion of the VSOP survey sample (Hirabayashi et al. 2000) with declinations $< 10^\circ$. The original sample is defined by: $S_{5\text{GHz}} > 0.95$ Jy, $\alpha < 0.45$, $|b| > 10^\circ$. Taking into account the further constraint $\delta < 10^\circ$, we estimate that the area covered is ~ 5 sr. The selected sources have $\alpha_{\text{thin}} > 0.5$ and spectral curvature $\alpha_{\text{thin}} - \alpha_{\text{thick}} > 0.6$.

We have excluded from the sample the gravitationally lensed source J0414 + 0534 because our models do not include the effect of lensing, and J1522 – 2730, classified as a BL Lac object, whose variability properties suggests that it is less likely to be a truly GPS source (Edwards & Tingay 2004). This leaves 7 GPS galaxies (5 having spectroscopic redshifts), 16 quasars (15 with spectroscopic redshift), and 2 empty fields (see Table 6).

3.6. The Parkes half-Jy sample

Snellen et al. (2002) selected from the Parkes multifrequency survey data in a region of about 3.9 sr a south-

Table 7. The Parkes half-Jansky sample of GPS galaxies (Snellen et al. 2002). The * denotes photometric redshift estimates.

Name	m_R	z	ν_p GHz
J0022+0014	18.10	0.305	0.6
J0108-1201	22.39	1.0*	1.0
J0206-3024	21.00	0.65*	0.5
J0210+0419	24.1	1.5*	1.3
J0210-2213	23.52	1.4*	1.5
J0242-2132	17.10	0.314	1.0
J0323+0534	19.20	0.37*	0.4
J0401-2921	21.0	0.65*	1.0
J0407-3924	20.40	0.54*	0.4
J0407-2757	21.14	0.68*	1.5
J0433-0229	19.10	0.36*	0.4
J0441-3340	21.0	0.65*	1.2
J0457-0848	20.30	0.52*	0.4
J0503+0203	21.0	0.583	2.5
J0943-0819	17.50	0.228	0.4
J0913+1454	20.0	0.47*	1.1
J1044-2712	21.0	0.65*	0.8
J1057+0012	21.0	0.65*	1.6
J1109+1043	20.50	0.55*	0.5
J1110-1858	19.60	0.497	1.0
J1120+1420	20.10	0.362	0.4
J1122-2742	21.0	0.65*	0.8
J1135-0021	16.50	0.16*	0.4
J1203+0414	18.80	0.33*	0.4
J1345-3015	21.0	0.65*	2.5
J1347+1217	15.20	0.122	0.4
J1350-2204	20.93	0.63*	0.4
J1352+0232	20.00	0.47*	0.4
J1352+1107	21.0	0.65*	3.6
J1447-3409	21.00	0.65*	0.5
J1506-0919	19.70	0.43*	0.6
J1521+0430	22.10	1.296	1.0
J1543-0757	17.40	0.172	0.4
J1546+0026	20.10	0.556	0.6
J1548-1213	21.88	0.883	0.4
J1556-0622	22.20	0.94*	0.4
J1604-2223	18.75	0.141	0.6
J1640+1220	21.36	1.150	0.4
J1648+0242	21.0	0.65*	3.4
J1734+0926	20.80	0.61*	1.0
J2011-0644	21.18	0.547	1.4
J2058+0540	23.40	1.381	0.4
J2123-0112	23.30	1.158	0.4
J2130+0502	22.21	0.990	1.0
J2151+0552	20.20	0.740	5.0
J2212+0152	22.0	0.88*	0.4
J2325-0344	23.50	1.4*	1.4
J2339-0604	22.91	1.2*	0.4

ern/equatorial sample of GPS sources with $S_{2.7\text{GHz}} > 0.5 \text{ Jy}$, excluding objects identified as quasars. The sample (see Table 7) consists of 49 objects with spectra peaking at $\nu_p > 0.4 \text{ GHz}$, 38 of which are identified with galaxies, 10 are too faint to be identified and 1 is too close to a

Table 8. The CORALZ sample of local GPS galaxies (Snellen et al. 2004).

Name	z	ν_p GHz
J073328+560541	0.104	0.460
J073934+495438	0.054	0.950
J083139+460800	0.127	2.200
J090615+463618	0.085	0.680
J131739+411545	0.066	2.300
J171854+544148	0.147	0.480

bright star to allow identification, and is excluded from the statistical analysis. The authors argue that, based on the magnitude distribution of other GPS samples, the 10 faint sources are unlikely to be quasars, and we assume them to be galaxies. Spectroscopic redshifts are available for 18 objects. Estimates, or lower limits, for the others have been obtained through Eq. (17). No restrictions on either the low- or the high-frequency spectral index are mentioned.

3.7. The CORALZ sample

The sample of Compact Radio sources at Low Redshift (CORALZ) was selected by Snellen et al. (2004) solely on the basis of the radio angular size ($\theta < 2''$), independent of radio spectra, picking out sources associated with relatively bright galaxies. It is estimated to be $\simeq 95\%$ complete for $S_{1.4\text{GHz}} > 100 \text{ mJy}$ over the redshift range $0.005 < z < 0.16$ in a region of 2850 square degrees. The sample comprises 6 GPS galaxies with $\nu_p > 0.4 \text{ GHz}$, all with spectroscopic redshifts (Table 8).

3.8. The WMAP survey

The WMAP point source catalogue (Bennett et al. 2003b) comprises 208 point sources with a $\geq 5\sigma$ detection in any of the 5 WMAP bands, in the range 22.8–93.5 GHz; 203 sources have counterparts in existing 4.85 GHz, the remaining 5 sources being probably spurious.

This is the first simultaneous multifrequency survey at mm wavelengths and is therefore well suited to select extreme HFPs. Although the completeness limit is at $S_{22.8\text{GHz}} \simeq 1.25 \text{ Jy}$ (De Zotti et al. 2005), to avoid that the estimates of spectral indices are too affected by measurement errors we have confined ourselves to sources with $S_{22.8\text{GHz}} \geq 2 \text{ Jy}$, and we have picked out those with inverted spectrum ($\alpha < 0$) from 22.8 to 33 GHz and from 4.85 to 22.8 GHz. There are 18 sources satisfying these criteria, a number close to the prediction of the De Zotti et al. (2000) model, for a maximum initial peak frequency of 200 GHz. Most of these sources are well known calibrators and have therefore many observations at many frequencies (see Trushkin 2003). They all show strong variability, consistent with that observed for blazars (see Tinti 2005); 9 of them are classified as blazars by Terasranta et al. (1998) or

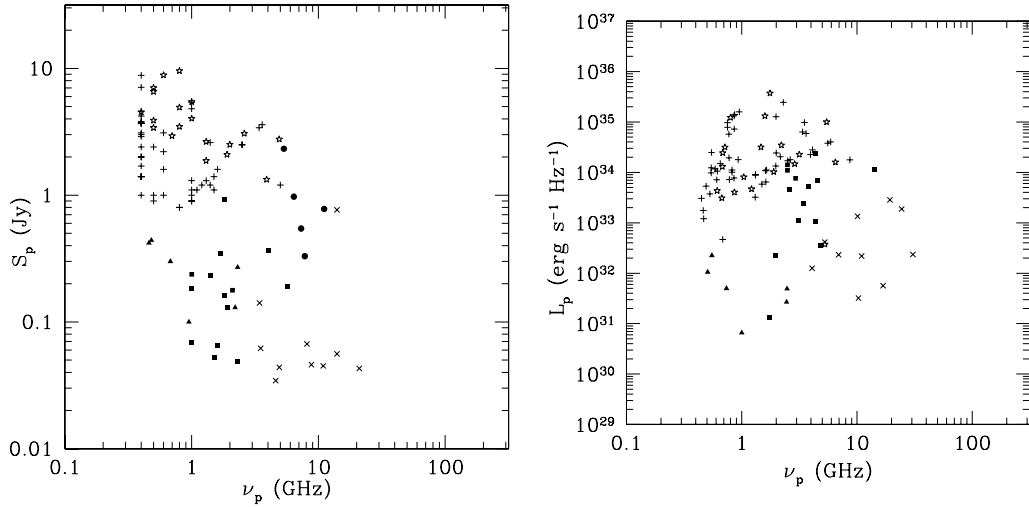


Fig. 1. Peak flux density versus observed peak frequency (left) and peak luminosity versus rest frame turnover frequency (right) for GPS galaxies in the various samples. HFP: filled circles; Bolton sample A: \times ; WENSS: filled squares; CORALZ: filled triangles; Stanghellini: \star ; Parkes: $+$.

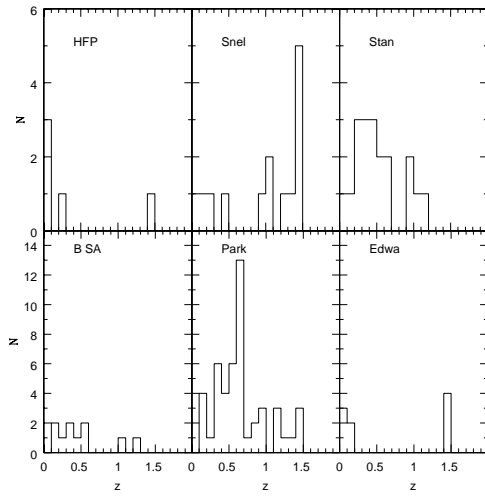


Fig. 2. Distributions of measured and estimated redshifts for the HFP, Stanghellini et al. (1998), Snellen et al. (1998), Bolton et al. (2004, sample A), Parkes, and ATCA GPS galaxy samples. Note that the peaks at $z = 1.5$ are due to unidentified sources, assumed to be galaxies at that redshift.

Donato et al. (2001). The data on the WMAP sample thus confirm that most quasars showing a peak at tens of GHz are likely blazars caught during a phase when a flaring, strongly self-absorbed synchrotron component dominates the emission spectrum (Tinti et al. 2005).

4. Impact of different selection criteria

The observational properties that generally define the different samples are:

- the flux density at the frequency of selection;

Table 9. Median values of the optically thick and thin spectral indices for the various samples.

Sample	α_{thick}	α_{thin}
HFP	-0.86	0.61
Stan	-0.76	0.67
B_SA	-0.38	0.76
B_SB	-0.43	0.82
Snel	-0.67	0.64

- the turnover frequency range;
- the spectral index in the optically thin and thick parts of the spectrum.

To effectively explore the luminosity and peak frequency evolution of GPS sources, we need samples that provide a wide coverage of the $\nu_p - S_p$ plane. The coverage provided by the present samples is shown in Fig. 1. HFP sources (Dallacasa et al. 2000) have turnover frequencies greater than 4.9 GHz, at or above the upper limits of the samples of Stanghellini et al. (1998) and Snellen et al. (1998, 2002, 2004). Because of their high selection frequency, 15 GHz, the Bolton et al. (2004) samples explore the high peak frequency region.

The samples by Bolton et al. (2004) have flux limits similar to the faint GPS sample selected by Snellen et al. (1998), although at a very different frequency, while the HFP and the Stanghellini et al. (1998), and the Parkes samples contain bright sources.

The redshift distributions of the galaxies in the various samples are shown in Fig. 2. Many redshifts are estimated from optical magnitudes. The peak at $z = 1.5$ is mostly due to optically unidentified GPS sources, assumed, following Snellen et al. (2000), to have that redshift.

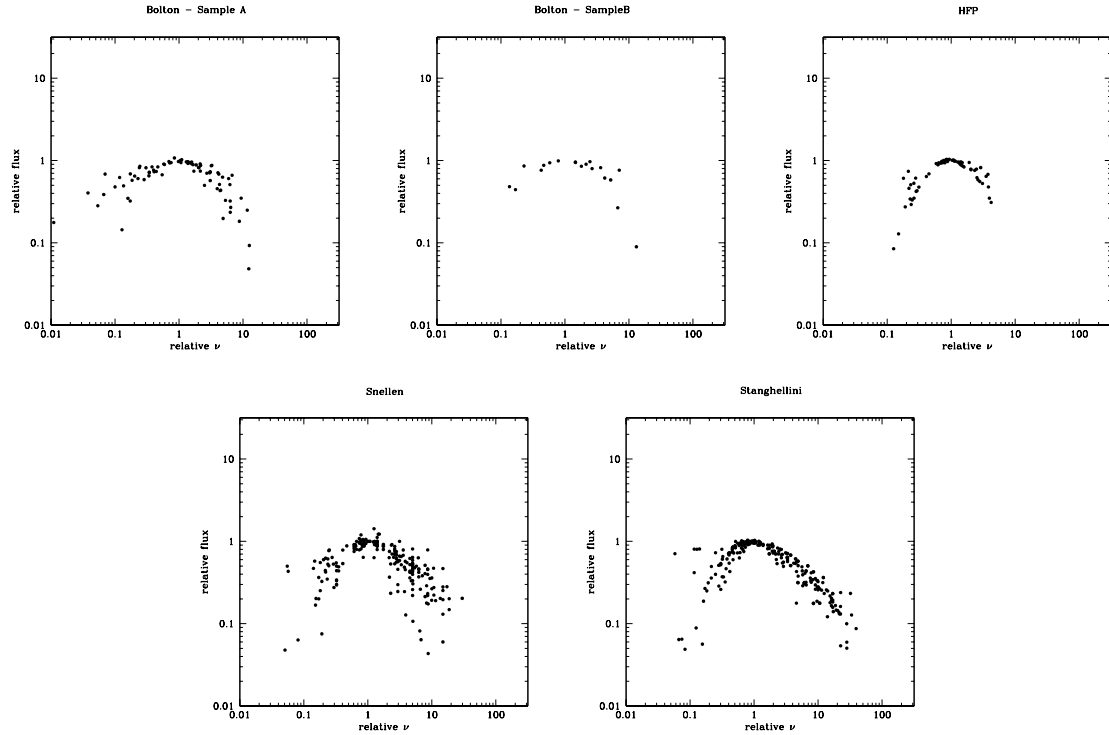


Fig. 3. Spectra of GPS sources in the various samples, normalized in both frequency and flux density.

As noted above, selection criteria include constraints on the spectral indices in the optically thick and/or in the optically thin spectral region. Stanghellini et al. (1998) required $\alpha_{\text{thin}} \geq 0.5$, Dallacasa et al. (2000) demanded $\alpha_{\text{thick}} \leq -0.5$; Edwards & Tingay (2004) applied both constraints. For other samples, the adopted spectral criteria are less explicit. Snellen et al. (1998, 2000) require an inverted spectrum at low frequencies and that the Full Width at Half Maximum of the spectrum is less than 2 decades in frequency; the latter condition implies that, typically, α_{thin} and $-\alpha_{\text{thick}}$ are ≥ 0.3 , a somewhat less restrictive constraint than adopted for the previously mentioned samples. An even looser criterion was adopted by Bolton et al. (2004): $\alpha_{1.4}^{4.8} < -0.1$. Not many details are given on spectral criteria for the Parkes sample (Snellen et al. 2002), while the CORALZ sample (Snellen et al. 2004) was selected on the basis of radio morphology, not of the spectra.

In Fig. 3 we compare the shapes of the radio spectra of the sources in the different samples, normalized to the peak frequencies and to the peak flux densities. It is apparent, and quantified in Table 9, that the median α_{thick} of Bolton et al. (2004) sources is considerably flatter than for the other samples. To homogenize this sample to the others, we have dropped sources with $\alpha_{\text{thick}} > -0.5$.

5. Results

We have fitted separately the redshift and the observed peak frequency, $\nu_{p,0}$, distributions of GPS galaxies in the samples described above. The best fit values of the pa-

Table 10. Best fit values of the model parameters for GPS galaxies.

$\log(n_0)$ [Mpc $^{-3}$ (d log L_ν) $^{-1}$ GHz $^{-1}$]	-14.13
β	0.83
$\log(\nu_{p,i})$ (GHz)	2.98
η	1.20
λ	0.0125

rameters have been obtained minimizing the chi-square function with the Minuit package (CERN libraries). We need to determine:

- the parameters characterizing the luminosity function, i.e. the normalization n_0 and the slope β ; the minimum and maximum luminosities, L_{\min} and L_{\max} respectively, both referred to the frequency of 300 MHz, below the conventional minimum peak frequency of GPS sources, have been set at the minimum and maximum observed values: $L_{\max}(300\text{MHz}) = 5 \cdot 10^{35} \text{ erg s}^{-1} \text{ Hz}^{-1}$, $L_{\min}(300\text{MHz}) = 10^{29} \text{ erg s}^{-1} \text{ Hz}^{-1}$;
- the slope, η , of the power-law dependence of the emitted radio power on source age;
- the slope, λ , of the power-law dependence of the peak frequency on source age;
- the initial value of the peak frequency, $\nu_{p,i}$;
- the redshift of formation of the first peaked spectrum sources, z_f ;

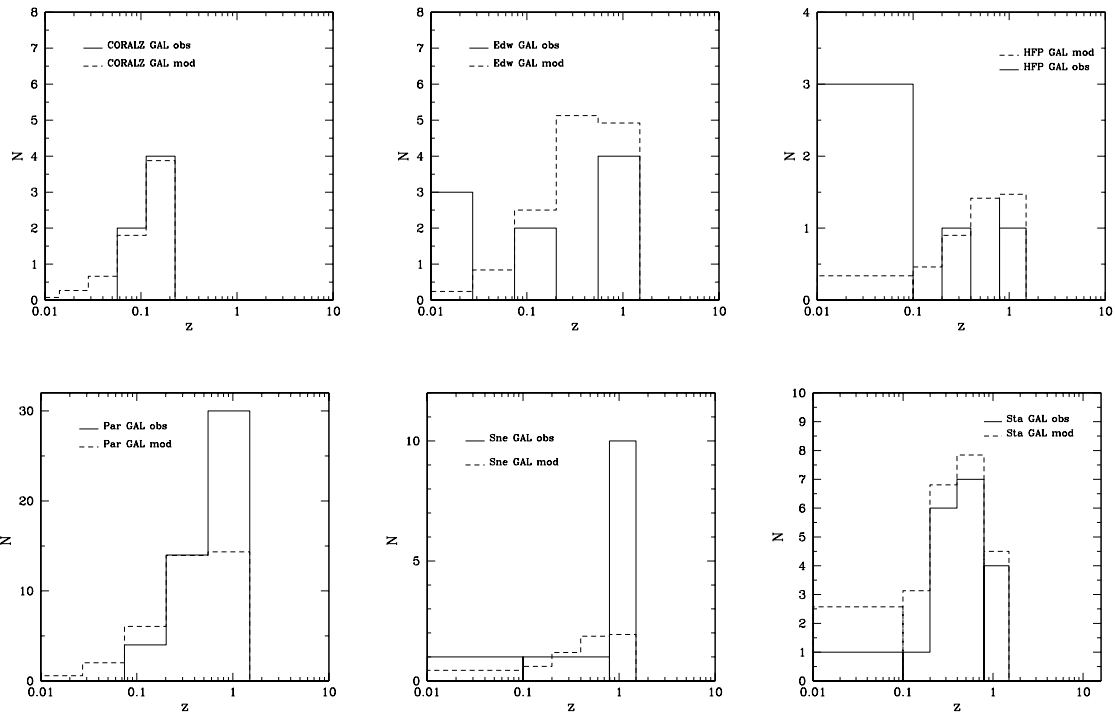


Fig. 4. Comparison of the redshift distributions yielded by the best fit model (dashed) with the observed ones (solid).

- the parameter k characterizing the cosmological evolution of the luminosity function.

We have checked that the data do not require cosmological evolution of the luminosity function of GPS galaxies, confirming the finding of De Zotti et al. (2000), and we have therefore set $k = 0$. We thus have $L_*(z) = \text{const} = L_0 = 10^{32} \text{ erg s}^{-1} \text{ Hz}^{-1}$ [Eq. (6)]. The fit is also insensitive to the value of z_f , provided that it is larger than the maximum estimated redshift of GPS galaxies in the considered samples. We have therefore fixed $z_f = 1.5$.

Figures 4 and 5 compare the model with the observed redshift and peak frequency distributions. The overall agreement is reasonably good, indicating that the underlying scenario is consistent with the current data.

The best fit values of the parameters are given in Table 10. The formal errors on them derived from the χ^2 statistics are rather small, but we regard them as unrealistic in view of the many uncertainties due to the difficulties in the sample selection; also the redshift distributions are largely built using photometric redshift estimates rather than spectroscopic measurements. Thus we prefer not to report uncertainties that are likely to be deceitful. That the real uncertainties are probably large is indicated by a comparison of the present best-fit values of the parameters with those found by De Zotti et al. (2000) analyzing some of the samples considered here. In particular, the values of η and λ are widely different [the difference of n_0 follows from that of λ , see Eq. (5)]. Still both analyses find positive values of η and negative values of $p = -\eta + \alpha\lambda$, implying that both the emitted radio power and the peak

luminosity *decrease* with increasing source age, at variance with the evolution models by Snellen et al. (2000) and Alexander (2000).

The slope of the luminosity function is more stable: we find $\beta = 0.83$ while De Zotti et al. (2000) found $\beta = 0.75$. Both values are not far from the slope of the low luminosity portion of the luminosity function of steep spectrum radio sources, $\beta_{ss} \simeq 0.69$ (Dunlop & Peacock 1990; Magliocchetti et al. 2002).

6. Discussion and conclusions

Although new samples have substantially improved the coverage of the luminosity–redshift–peak frequency space of GPS galaxies, the assessment of their evolutionary properties is still difficult. First of all, there is no fully agreed set of criteria to ascertain whether a source is truly a GPS. The frequently adopted GPS identification conditions rely on the spectral shape. However, as mentioned in Sects. 3 and 4, different spectral requirements have been adopted by different groups and recovering a homogeneous set of data is not easy and may be even impossible. Other properties that GPS sources should have, include a compact structure (size $\lesssim 1$ kpc), low polarization, low variability, and sub-luminal component motions. Regrettably, measurements of these quantities are available only for a limited number of GPS candidates. The samples we are using may therefore be contaminated by sources of different nature.

Also, a significant fraction of objects are still unidentified, and spectroscopy of identified objects is highly in-

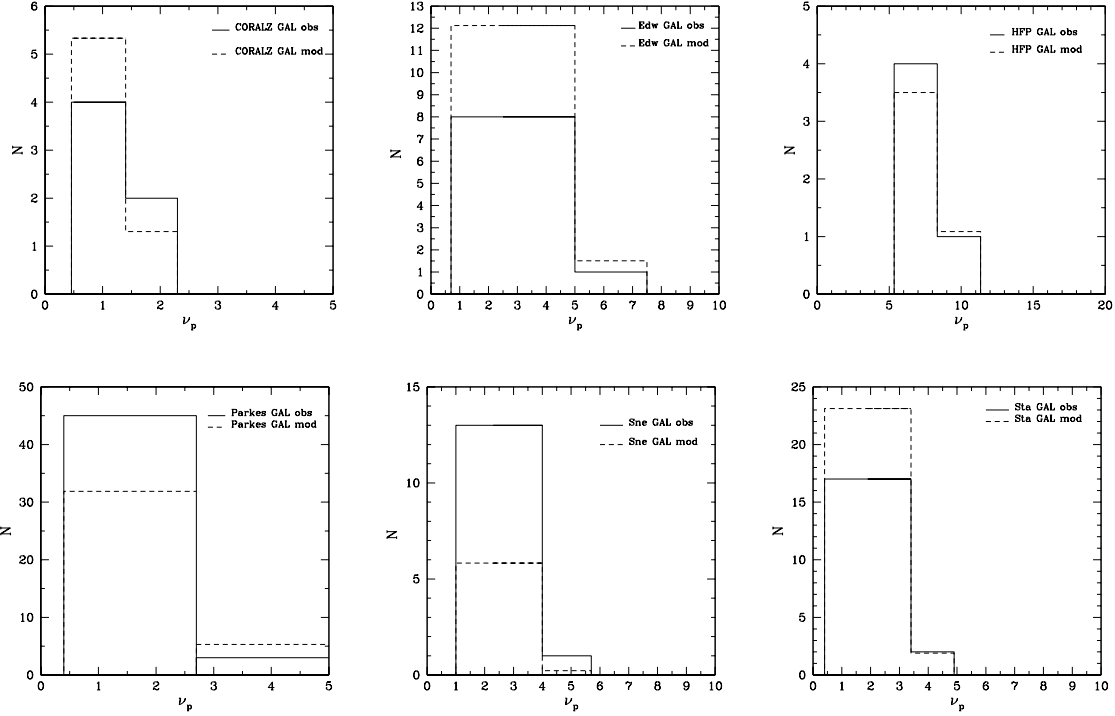


Fig. 5. Comparison of the peak frequency distributions yielded by the best fit model (dashed) with the observed ones (solid).

complete, so that many redshifts are estimated from optical magnitudes. Although GPS galaxies seem to have a rather well defined redshift–magnitude relationship, its dispersion is significant and may increase with redshift.

With these premises we cannot expect to be able to come out with a clear assessment of the evolutionary properties of GPS galaxies. Still, some interesting conclusions can be drawn. First, the simple luminosity evolution scenario for individual sources outlined in Sect. 2 appears to be fully consistent with the data. We note however that, although the formalism stems from the self-similar evolution models by Fanti et al. (1995) and Begelman (1996, 1999), according to which both the parameters η and λ are determined by the slope n of the density profile of the ambient medium, the data can be satisfactorily fitted only if the two parameters are treated as independent. This is not surprising, since self-similarity can be easily broken under realistic conditions, and indeed deviations from self-similarity were found in the two-dimensional hydrodynamical simulations of Carvalho & O’Dea (2002).

The fit is obtained for a positive value of η and a negative value of p , implying a decrease of the emitted power and of the peak luminosity with source age or with decreasing peak frequency, at variance with the Snellen et al. (2000) model. On the other hand, our analysis confirms the rather flat slope of the luminosity function, found by Snellen et al. (2000) who also report indications of a high luminosity break, not required by the data sets we have used. Snellen et al. (2000) argue that, in the framework of a scenario whereby GPS sources increase their

luminosity until they reach a size ~ 1 kpc and dim thereafter, during the CSS and extended radio source phases, the luminosity function of GPS galaxies can evolve into that extended radio sources. Our results suggest that the GPS galaxies are the precursors of extended radio sources with luminosities below the break of the luminosity function ($L_{\text{break}} \sim 10^{33} \text{ erg s}^{-1} \text{ Hz}^{-1}$ at 2.7 GHz, cf. Dunlop & Peacock 1990, De Zotti et al. 2005). Our best fit model implies that the source luminosity is, roughly, inversely proportional to the source age. If GPS sources have typical ages of $\simeq 10^3$ yr and extended radio sources of $\simeq 10^7$ yr, we expect the latter to be $\sim 10^4$ times less powerful than the former; as shown by Fig. 1, the maximum value of the peak luminosity we found is $\sim 10^{36} \text{ erg s}^{-1} \text{ Hz}^{-1}$ (but this may be a lower limit, since we have arbitrarily set the maximum redshift at $z_f = 1.5$), i.e. about 3 orders of magnitude larger than L_{break} . The GPS sources in the samples considered here are thus expected to evolve into large-scale radio galaxies with $L < L_{\text{break}}$.

It must be stressed, however, that the uncertainties are very large, so that firm conclusions must await for larger samples and more complete redshift information. In particular, we have checked that still acceptable fits can be obtained setting the exponent η of the relationship between the emitted radio power and the source age to the value implied by Begelman’s model for $n = 2$, i.e. $\eta = 0.5$ (the total χ^2 increases by $\delta\chi^2 \simeq 2$). In this case, the source luminosities would typically decrease by a factor of ~ 100 from the GPS to the extended radio source phase, and GPS sources could be the progenitors of extended radio

sources with luminosities both above and below L_{break} . It is plausible that sources have a distribution of values of η whereby the lower values become increasingly rare, to account for the steepening of the luminosity function above L_{break} . Alternatively, the fraction of prematurely fading sources may increase with luminosity. If $\eta = 0.5$, the best fit value of λ is 1.02, and the peak luminosity, $L_p(\nu_p)$ *increases*, albeit slowly, with *decreasing* peak frequency [$L_p(\nu_p) \propto \nu_p^{-0.25}$, cf. eq. (3)]. The other values of the parameters keep values very close to those in Table 10.

Another key observable quantity potentially providing crucial constraints on evolutionary models is the linear size. The self-similar evolution models predict its dependence on source age, given the density profile of the ambient medium, and on the other fundamental observable, the radio power. However, as noted above, we could not fit the data with strictly self-similar models, so that we no longer have a well defined relationship between radio power and linear size. Such a relationship, however, can be recovered through the *observed* relationship between turnover frequency and linear size, $\nu_p \propto l^{-\delta}$, with $\delta \simeq 0.65$; we have $L \propto l^{-\eta\delta/\lambda}$. The anticorrelation between the latter quantities implies that, since the radio power *decreases* with decreasing peak frequency, it decreases with increasing linear size. Once again, however, the uncertainties are very large. The formal best fit values of the parameters would imply an unrealistically steep decrease of the radio power, L , with increasing linear size, l , but, if $\eta = 0.5$, $L \propto l^{-0.32}$ and $L_p(\nu_p) \propto l^{p\delta/\lambda} \propto l^{0.17}$.

In turn, fixing the exponent λ of the relationship between peak frequency and source age to the value implied by Begelman's model for $n = 2$, i.e. $\lambda = \delta = 0.65$, we get again an increase of the minimum χ^2 by $\delta\chi^2 \simeq 2$, the best fit value of η is 0.76, while the other parameters are essentially unchanged. In this case we have $L_p(\nu_p) \propto \nu_p^{0.42}$, $L \propto l^{-0.76}$, and $L_p(\nu_p) \propto l^{-0.27}$.

These examples illustrate the importance of the determination of linear sizes for large complete samples of GPS sources. Given their extreme compactness and their redshift distribution, images with milli-arcsec resolution are generally required. It is thus not surprising that the currently available information is scanty and inhomogeneous. New VLBA data are however being acquired and analyzed, for example on the HFP sample (Orienti et al. 2005). Future evolutionary models should comply also with the distributions of linear sizes and with relationships of sizes with radio power.

Complementary information on the proposed evolutionary sequence linking GPS sources to large scale radio sources is provided by CSS sources, which could correspond to the intermediate phase when sources have expanded out of the narrow line region but are still within the host galaxy. More complete evolutionary studies should take into account also these sources.

Acknowledgements. We warmly thank Daniele Dallacasa for useful discussions and suggestions. This work has made use of the NASA/IPAC Extragalactic Database NED which is oper-

ated by the JPL, California Institute of Technology, under contract with the National Aeronautics and Space Administration. The authors acknowledge financial support from the Italian ASI and MIUR.

References

Alexander, P. 2000, MNRAS, 319, 8
 Baum, S.A., O'Dea, C.P., de Bruyn, A.G., et al. 1990, A&A, 232, 19
 Begelman, M.C. 1996, in Proc. "Cygnus A - Study of radio Galaxy", Carilli C.L. & Harris D.E. eds., CUP, Cambridge, p. 209
 Begelman, M.C. 1999, in The Most Distant Radio Galaxies, proc. of the KNAW colloquium held in Amsterdam, 15-17th October 1997, eds. H.J.A. Röttgering, P.N. Best, M.D. Lehnert, KNAW, Amsterdam, p. 173
 Bennett, C.L., Halpern, M., Hinshaw, G., et al. 2003a, ApJS, 148, 1
 Bennett, C.L., Hill, R.S., Hinshaw, G., et al. 2003b, ApJS, 148, 97
 Bicknell, G.V., Dopita, M.A., & O'Dea, C.P.O. 1997, ApJ, 485, 112
 Bolton, R.C., Cotter, G., Pooley, G.G., et al. 2004, MNRAS, 354, 485
 Carvalho, J.C., & O'Dea, C.P. 2002, ApJS, 141, 371
 Conway, J.E. 2002, NewAR, 46, 263
 Dallacasa, D., Falomo, R., & Stanghellini, C. 2002a, A&A, 382, 53
 Dallacasa, D., Stanghellini, C., Centonza, M., et al. 2000, A&A, 363, 887
 De Zotti, G., Granato, G.L., Silva, L., Maino, D., & Danese, L. 2000, A&A, 354, 467
 de Zotti, G., Ricci, R., Mesa, D., Silva, L., Mazzotta, P., Toffolatti, L., & González-Nuevo, J. 2005, A&A, 431, 893
 Donato, D., Ghisellini, G., Tagliaferri, G., & Fossati, G. 2001, A&A, 375, 739
 Dunlop, J.S., & Peacock, J.A. 1990, MNRAS, 247, 19
 Edwards, P.G., & Tingay, S.J. 2004, A&A, 424, 91
 Fanti, C., Fanti, R., Dallacasa, D., et al. 1995, A&A 302, 317
 Fanti, R., Fanti, C., Schilizzi, R.T., et al. 1990, A&A, 231, 333
 Fukugita, M., Shimasaku, K., & Ichikawa, T. 1995, PASP, 107, 945
 Hirabayashi, H., Fomalont, E.B., Horiuchi, S., et al. 2000, PASJ, 52, 997
 Magliocchetti, M., Maddox, S.J., Jackson, C.A., et al. 2002, MNRAS, 333, 100
 O'Dea, C.P. 1998, PASP, 110, 493
 O'Dea, C.P., & Baum, S.A. 1997, AJ, 113, 148
 Orienti, M., Dallacasa, D., Tinti, S., & Stanghellini, C. 2005, in preparation
 Readhead, A.C.S., Taylor, G.B., Pearson, T.J., & Wilkinson, P.N. 1996, ApJ 460, 634
 Snellen, I.A.G., Bremer, M.N., Schilizzi, R.T., Miley, G.K., & van Ojik, R. 1996, MNRAS, 279, 1294
 Snellen, I.A.G., Lehnert, M.D., Bremer, M.N., & Schilizzi, R.T. 2002, MNRAS, 337, 981
 Snellen, I.A.G., Mack, K.-H., Schilizzi, R.T., & Tschager, W. 2004, MNRAS, 348, 227
 Snellen, I.A.G., Schilizzi, R.T., de Bruyn A.G., et al. 1998, A&AS 131, 435
 Snellen, I.A.G., Schilizzi, R.T., Miley, G.K., et al. 2000, MNRAS, 319, 445

Teräranta, H., Tornikoski, M., Mujunen, A., et al. 1998,
A&AS, 91, 121

Tingay, S.J., Edwards, P.G., & Tzioumis, A.K. 2003, MNRAS,
346, 327

Tinti, S. 2005, Ph.D. thesis, SISSA/ISAS, Trieste

Tinti, S., Dallacasa, D., de Zotti, G., Celotti, A., &
Stanghellini, C. 2005, A&A, 432, 31

Torniainen, I., Tornikoski, M., Teräranta, H., Aller, M.F., &
Aller H.D. 2005, A&A, 435, 839

Trushkin, S.A. 2003, Bull. Spec. Astrophys. Obs. N. Caucasus,
55, 90, astro-ph/0307205